Nanofabrication by self-assembly

The self-assembly paradigm in chemistry, physics and biology has matured scientifically over the past two-decades to a point of sophistication that one can begin to exploit its numerous attributes in nanofabrication. In what follows we will take a brief look at current thinking about self-assembly and with some recent examples taken from our own work examine how nanofabrication has benefited from self-assembly.

Geoffrey A. Ozin[1,*], Kun Hou[1], Bettina V. Lotsch[2], Ludovico Cademartiri[3], Daniel P. Puzzo[1], Francesco Scotognella[4], Arya Ghadimi[1] and Jordan Thomson[1]

[1]Materials Chemistry Research Group, Chemistry Department, 80 St. George Street, University of Toronto, Toronto, Ontario, Canada M5S3H6

[2]Department of Chemistry and Biochemistry, Ludwig Maximilian University, Butenandtstraße 5-13, Haus D, 81377 Munich, Germany

[3]Department of Chemistry and Chemical Biology, Harvard University, 12 Oxford Street, Cambridge, MA, 02138

[4]Department of Materials Science, Università of Milano Bicocca, Via Roberto Cozzi 55, 20125 Milan, Italy

*Email: gozin@chem.utoronto.ca

There have been spectacular advances in our scientific understanding of the forces that control self-assembly since the phenomenon was first recognized, and given that name about half a century ago. Today it is widely appreciated that the forces that drive the self-assembly of molecules and colloids, materials and polymers into an organized structure or pattern must be expanded beyond those responsible for conventional ionic, covalent, metallic, hydrogen and coordination bonds to include weaker interactions, like van der Waals and Casimir, π-π and hydrophobic, colloidal and capillary, convective and shear, magnetic, electrical and optical forces. Armed with self-assembly as a synthetic tool, powerful chemistry protocols can be developed that are capable of organizing organic and inorganic building-blocks into unprecedented structures and patterns, over several length scales to create novel kinds of integrated chemical, physical and biological systems, which pose myriad of opportunities in nanotechnology. In this article we will briefly examine the physicochemical underpinnings of self-assembly and describe how self-assembly has enabled the practical realization of some nanofabrication objectives by reference to recent examples from our research: a nanoparticle photonic crystal dye laser, three-dimensional nanocrystal and nanowire architectures, an antibacterial silver Bragg mirror and a dye-anchored mesoporous metal oxide electrochemiluminescent device.

What is self-assembly – what are its roots?

The 'assembly' connotes 'to put together or build' and the 'self' implies 'without outside help or on its own'. So we are talking about structures and patterns, large and small that put themselves together from basic building blocks in a parallel manner, exemplified by living organisms and galaxies.

The Greek philosopher Democritus in 400 BC imagined all matter in the universe evolved from the organization of atomistic components to form the Earth and solar system, stars and galaxies[1]. The French philosopher Descartes two millennia later envisioned an ordered universe arising out of chaos according to natural laws through the organization of small objects into larger assemblages[1]. The language of Democritus

and Descartes seems to be synonymous with our current thinking about self-assembly whereby a system of initially disordered components spontaneously organizes to a more ordered one without direction by an external influence. Incidentally, these two philosophers are regarded as among the leading philosophical influences of science. Thinking of this kind can be considered to have inspired later theories that explain self-organizing systems in physics and mathematics, biology and chemistry.

On a different level, the exploration of the biological world soon showed how the most sophisticated structures made by Nature are often obtained by the assembly of molecular sized construction units. While, in a sense, Nature showed us from the beginning how self-assembly is done, it took us quite a long time to recognize it.

In the framework of nanofabrication by bottom-up synthetic chemistry, self-assembly has provided a powerful way of making materials and organizing them into functional constructs designed for a specific purpose. Self-assembly, as a fundamental building principle, teaches that matter of all kinds, exemplified by atoms and molecules, colloids and polymers, can undergo spontaneous organization to a higher level of structural complexity, driven by a map of forces operating over multiple length scales.

The origin of today's self-assembly seems to be a natural outgrowth of a confluence of ideas taken from the work of Langmuir and Blodgett[2] in 1935 on the formation of close-packed arrangements of amphiphilic molecules on liquid and solid surfaces and observations of Bigelow et al.[3] in 1946 that long chain alkylamines form a densely packed monolayer on the surface of platinum. While there was no explicit mention of the term self-assembly to explain the formation of well-ordered molecular monolayers it is clear that self-assembly was operating in these systems. In 1983 Nuzzo and Allara contacted gold surfaces with alkyl disulfides and discovered they formed close-packed monolayers of chemisorbed alkanethiolate molecules, called self-assembled monolayers (SAMs)[4-6].

What is nanofabrication?

Nanotechnology in its broadest terms refers to devices with dimensions in the range of 1 to 100 nm while nanofabrication involves the manipulation of matter at the nanoscopic length scale to provide by design structures and patterns with purposeful function that enable nanotechnology.

These days matter can be shaped, positioned and organized at the nanoscale using two approaches which have been dubbed top-down and bottom-up nanofabrication. The former involves the use of ion and electron, photon and atom beams to sculpt matter from macroscopic to nanoscopic dimensions in a serial process to form functional constructs with purposeful utility while the latter self-assembles these constructs in a parallel manner from nanoscale building blocks.

The self-assembly paradigm in chemistry and physics, materials science and engineering, biology and medicine has matured scientifically over the past two-decades to a point of sophistication that one can

exploit its numerous attributes in nanofabrication. Nowhere is its potential for nanofabrication better appreciated than in the self-assembly of alkanethiol monolayers on gold for a myriad of soft-lithographies[7, 8], layer-by-layer electrostatic self-assembly of polyelectrolytes of alternating charge for smart drug delivery vehicles[9-11], bio-conjugated self-assembled nanocrystals for medical diagnostics[12, 13], self-assembled semiconductor nanowires for flexible electronics[14, 15], self-assembled microspheres for opal optics[16], periodic mesoporous carbons for lithium solid state battery anodes[17], and microphase separated block copolymers as nanolithographic masks for silicon-based flash memories[18].

These are but a few high profile examples of how self-assembly has been an enabler of nanofabrication and a facilitator of nanotechnology. In what follows we will take a brief look at current thinking about self-assembly and with some recent examples taken from our own work examine how nanofabrication has benefited from self-assembly.

Pinning down self-assembly

Arriving at a scientific consensus about 'what self-assembly is' has been a hard task since its terminology and practice cross the boundaries between fields, traverse multiple length scales and span a range of forces; fields as diverse as cosmology and biology, length scales from nanoscopic to macroscopic, forces from 'weak' to 'strong'[19]. Nature shows control of self-assembly from cosmological length scales down to the atomic and subatomic length scales. Depending on interpretations, humans can control self-assembly on a much more limited range: from the atomic scale to the meter scale.

The term self-assembly implies spontaneity, a structure builds itself from modular construction units, an ordered pattern forms from a disordered state. The self that drives the assembly is the interaction among the building blocks rather than the generally stronger bonding force within them.

To self-assemble building blocks into well organized constructs depends on the ability to control their size, shape and surface properties to a high level of perfection. Therefore a prime goal of self-assembly is to synthesize building blocks with specified dimensions and form, and through chemical control of their surface properties (e.g., charge, hydrophobicity, hydrophilicity, functionality) gain command over the attractive and repulsive forces between them to allow them to assemble spontaneously over multiple length scales to create an integrated chemical, physical or biological system with purposeful function and utility[20].

In the absence of external influences, building block static self-assembly is driven by energy minimization to form static equilibrium structures. In the presence of outside influences, a dynamically self-assembling system may prevail that can adjust to its surrounding environment, by residing on an energetic minimum which is caused by the influx of energy in the system – once the energy stops flowing into the system, the minimum disappears and the system disassembles. Any living organism is a perfect example of dynamic self-assembly.
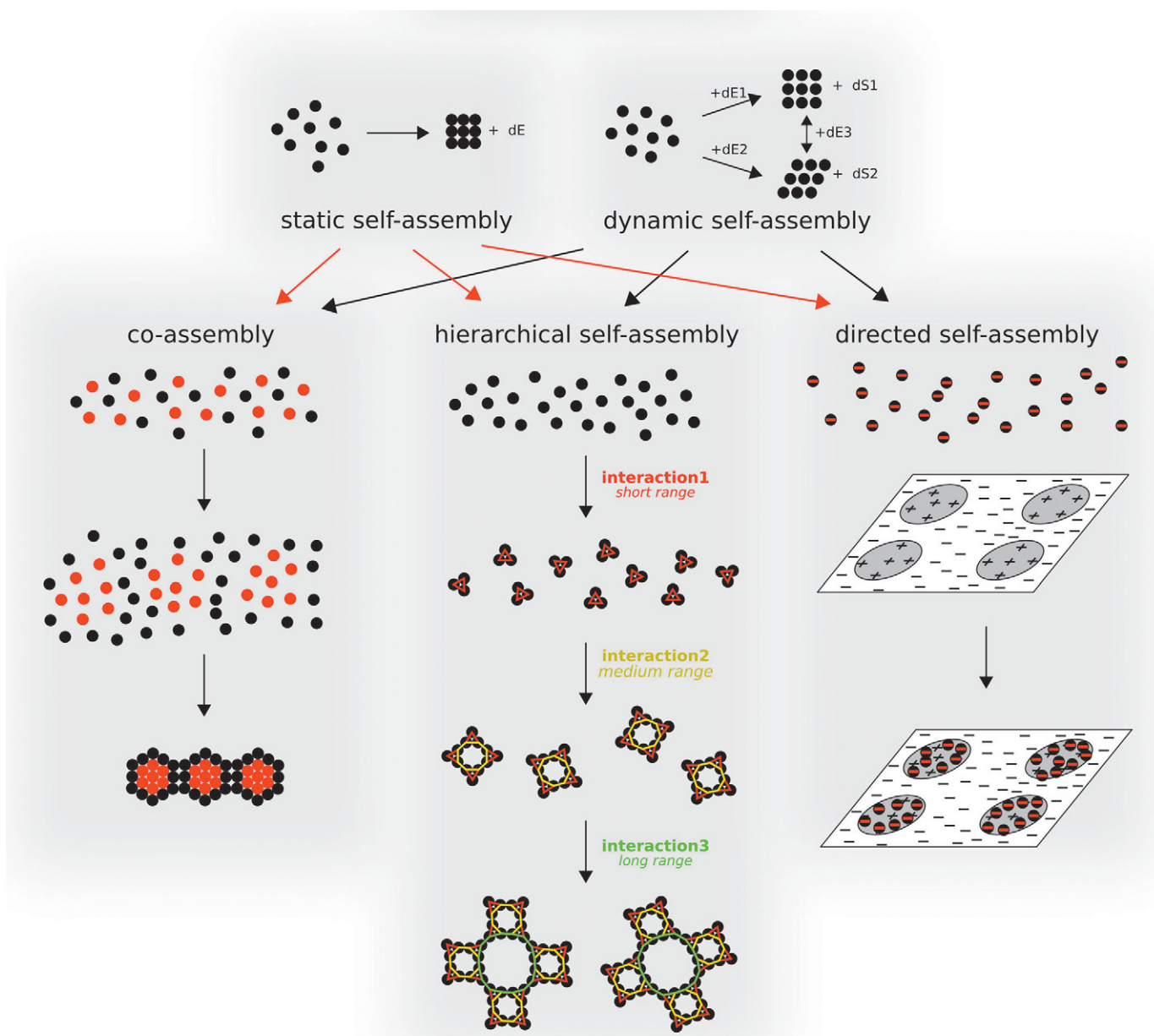
Fig. 1 Graphical rendition of static and dynamic self-assembly and how they relate to co-assembly, hierarchical assembly and directed assembly. This illustration is taken with permission from Concepts of Nanochemistry, L. Cademartiri and G.A.Ozin, VCH-Wiley, 2009[20].

It reduces entropy by absorbing energy from the environment. This gradient in entropy between the organism and the environment can be maintained only as long as energy is driven from the environment into the organism in the form of food and heat. Once that flux ceases, the organism disassembles. These two main categories of self-assembly called static and dynamic are illustrated in Fig. 1.

The processes of static and dynamic self-assembly can be further roughly sub-divided into co-assembly, directed self-assembly and hierarchical self-assembly as shown in Fig. 1. The dividing lines between these are blurred by mixed cases of directed co-assembly, directed hierarchical self-assembly or hierarchical co-assembly. Complex systems like the human organisms generally have aspects of all three categories, being examples of directed co-assembled hierarchical systems.

To amplify, co-assembly represents cases in which the simultaneous self-assembly of different building blocks within the same system leads to a synergic architecture that could not have been produced by the isolated self-assembly of either building block. An example of this

could be the formation of periodic mesoporous silicas by surfactant micelle templating of silicate building blocks[21]. While the kinetics of the individual assembly processes involved is still subject to debate, the overall process is synergic and, as such, it can be considered as a case of co-assembly.

Hierarchical self-assembly is characterized by the organization of a single building block over multiple length scales. The original building blocks organize into a 'first order' assembly, which becomes the building block for a larger 'second order' assembly. This process can lead to several orders of assembly. Biological systems are famous for employing this technique to create large functional structures out of molecular building blocks. In this sense biological systems are far superior to anything we have been able to design. An example of artificial hierarchical self-assembly could be opal film casting of lyotropic liquid crystal templated periodic mesoporous silica, boasting four length scales in one construct, from (i) the microscopic silica tetrahedral building units to (ii) the mesoscopically ordered porosity to (iii) the macroscopic air voids of the inverse opal replica and finally to (iv) the overall form of the inverse periodic mesoporous silica opal film[22].

Directed assembly is a case where the self-assembly is directed by external forces that had been placed by design. This is the typical case for bottom-up-meets-top-down approaches where a lithographic pattern can be used to direct the self-assembly of colloids from solution on a substrate[23]. Dip-pen nanolithography can also be considered as a case of directed self-assembly where the amphiphilic molecules self-assemble on a substrate but are directed by the liquid meniscus between the tip of the pen and the substrate[24].

These categories apply for both static and dynamic self-assembly. Dynamic self-assembly is more 'subtle' but potentially far more powerful than the static variety. One might think of it as a sub-class of self-assembly that creates stable but non-equilibrium structures and patterns which retain their order as long as the system continues to dissipate energy[25]. Dynamic order arises from opposing interactions between autonomously moving components that exist out of equilibrium and which can be altered by dissipating energy into the system. The system returns to equilibrium when the influx of energy stops. The kinetics of this disassembly process is strongly dependent on the specific system involved and has to be taken into consideration for fabrication purposes. The static self-assembly generates structures which are at equilibrium and are thus permanent, unless the environment is changed leading to a different equilibrium state.

Dynamic self-assembling systems, both living and non-living, involve collections of interacting building blocks that can adapt or react to a chemical or physical stimulus in their surroundings. Unlike the forces that drive building blocks to self-assemble into an organized static state as the system reduces its free energy and moves towards equilibrium, in dynamic self-assembly groups of interacting building blocks can arrange into structures and patterns away from thermodynamic equilibrium and

these patterns can be reconfigured by responding to external stimuli thereby making them adapt to their environment.

Dynamic self-assembly can be achieved in practice by changing an energy flux delivered to a system of building blocks interacting through opposing attractive and repulsive forces, an example being super-paramagnetic shaped objects floating at an air-liquid or liquid-liquid interface attracted by capillary forces and repelled by induced magnetic dipole forces, the latter being controlled by the magnitude of an externally applied magnetic field.

In any case of self-assembly, one of the fundamental consequences of self-assembly is the role of defects. Even in a most sophisticated example of dynamic self-assembly which is the human body, defects are ubiquitous. We evolve thanks to them, and survive *via* the purposely imperfect correction or tolerance of the lethal ones. While one has to distinguish between different kinds of errors and defects – and there is a myriad of different categories of 'defects' and 'errors' – we are here considering all those 'imperfections' of which self-assembly is so typically imbued.

This is, we feel, the greatest and for now insurmountable difference between what we could call 'rational device design' – which we use to make things – and 'life's design', which Nature used to make us. Our rational design is based on the elimination of defects, complexity, adaptability and evolution, on the directed assembly of every component, and measuring efficiency on the basis of speed and throughput. In short, if you cannot make it better, make it bigger and faster. Nature's design of organisms seems instead to be based on the promotion of defects and their correction when needed, on function brought by networks of large numbers of interacting and interdependent simple processes, on the hierarchical self-assembly from a small set of perfect and simple starting materials, and on measuring efficiency on the basis of energy and element efficiency as well as adaptability (parsimonious and frugal Nature).

Until this conceptual gap will start to be bridged even partially, but convincingly, we fear we will not see a radical shift of our manufacturing paradigms towards self-assembly.

Nanofabrication by self-assembly

In what follows we will illustrate the practice of nanofabrication through self-assembly using examples from our recent research, which employ the most diverse kinds of self-assembly. Our selection is intended to specifically highlight the importance of self-assembly as a repertoire of processes suitable to design various kinds of complex hierarchical structures with built-in functionality. The overall ensembles are typically made by a complex interplay of different kinds of self-assembly on different levels, which is oftentimes driven by external forces and directed by templates. Note that the functionality of these architectures is intrinsically linked to their hierarchical structure and their morphologies, which in turn are a consequence of a complex self-assembly history.
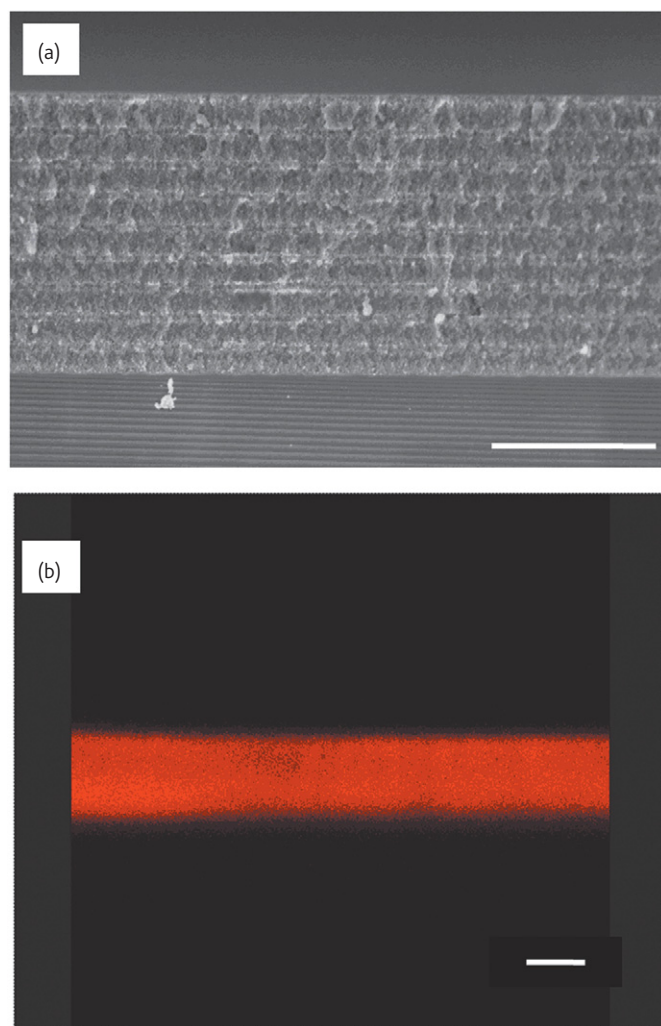
Fig. 2 (a) SEM image of a SiO_2/TiO_2 nanoparticle 1D PC (scale bar: 1 µm). (b) Confocal microscopy image showing the uniformity of the dye loaded throughout the constituent nanoparticle layers of the 1D PC (scale bar: 1.5 µm). Note that the thicknesses of the two images correlate well. Reproduced with permission of[26].

Nanoparticle photonic crystal dye laser

The hallmark of a dye laser[26] compared to a gas and solid state laser (e.g. argon ion and neodynium doped yttrium aluminum garnet) is that the lasing medium is a solution of an organic dye like Rhodamine 6G dissolved in an organic solvent. A feature of the dye laser is the broad emission of the dye which enables continuous wave or pulsed operation with tuning over a broad range of wavelengths. A disadvantage of this kind of liquid laser is that the dye solution has to be circulated from a large reservoir to avoid deleterious light induced degradation of the dye. Also the shaping and alignment of dye nozzles and their excitation are quite complicated. While changing the dye can generate different wavelengths with the same laser, this involves scrupulous cleaning of all components to remove all traces of the original dye and may also

necessitate changing optical components of the laser. All of this is pretty inconvenient for the laser operator.

A way to circumvent many of the problems associated with the conventional dye laser is to make it instead from all-solid-state components. This can be achieved in practice by integrating the colloidal assembly and dye adsorption properties of nanoparticles with the band-edge lasing attributes of photonic crystals[27-31].

A self-assembly approach for reducing such a solid-state dye laser to practice involves the steps of (i) evaporation induced self-assembly of alternating layers of colloidally stable dispersions of silica and titania nanoparticles into a 1D photonic crystal[32, 33], known as a Bragg mirror using slightly basic conditions to endow the surfaces of the nanoparticles with a negative charge, (ii) mechanical stabilization of the Bragg mirror by thermally induced necking of the nanoparticles, (iii) adsorption from solution of the cationic organic dye Rhodamine 6G onto the anionic surface of the nanoparticles, (iii) allowing the nanoparticle 1D photonic crystal dye laser to dry by solvent evaporation.

A scanning electron microscopy and confocal optical microscopy image of a cross-section of a representative 11-layer SiO_2-TiO_2 nanoparticle 1D photonic crystal is shown in Fig. 2 from which the uniformity of the constituent layers, quality of interfaces and uniformity of the adsorbed Rhodamine 6G throughout the layers can be appreciated.

This nanoparticle-based 1D photonic crystal possesses high reflectivity arising from Bragg diffraction of light incident on a photonic lattice comprised of layers of alternating refractive index and thicknesses fashioned on the scale of the wavelength of visible light. Most significantly, the nanoparticle layers imbue the photonic lattice with mesoporosity and high surface area thereby permitting the adsorption of a high loading of the fluorescent dye into the void spaces of the photonic crystal to enable operation of a low-threshold band edge laser.

By exciting the dye loaded nanoparticle 1D photonic crystal with a pump energy density of 40 µJ.cm^{-2}, as shown in Fig. 3a, it is possible to observe a narrow emission peak at 548 nm, which corresponds to the wavelength where the blue edge of the photonic stopband overlaps the tail of the Rhodamine 6G spontaneous emission, depicted in Fig. 3b. Reflectance and emission of the dye-loaded photonic crystal were collected parallel to the direction of the periodicity, taking into account the angular dependence of the photonic stopband. The observation of this phenomenon established that stimulated emission at 548 nm can be associated with the laser cavity created by the 1D photonic crystal, since the dye emission intensity is maximum at a wavelength of 570 nm[34, 35].

Photoluminescence spectra recorded below threshold show just the broadband emission of the organic dye, which is slightly modified by the photonic stopgap profile. However, once the sample is excited above the threshold excitation power, a narrow emission with about 8 nm full width at half maximum is obtained, corresponding to a cavity quality factor Q ~ 70. The measured full width at half maximum (FWHM) is
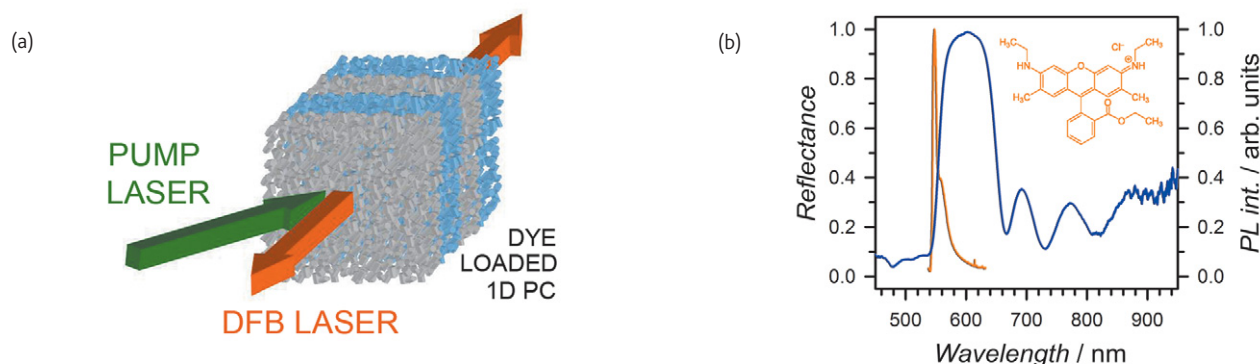
Fig. 3 *(a) Schematic representation of the optical configuration to obtain distributed feedback (DFB) laser emission from the nanoparticle 1D photonic crystal dye laser (b) Reflectance spectrum (blue line) and photoluminescence spectrum (orange line) of the dye loaded nanoparticle 1D PC excited by pulsed laser light at 532 nm with a energy density of 40 μJ.cm^{-2}. The inset shows the molecular structure of the R6G dye. Reproduced with permission of*[26].

comparable to values obtained with other dye doped 1D PC systems. A strong enhancement of the emission peak intensity with a concomitant rapid decrease in its full width at half maximum is observed with increasing excitation power density. Dye bleaching occurred at 0.6 J.cm^{-2} which is a density orders of magnitude higher with respect to the ones used in the experiment. Spectral line narrowing and increased emission intensity are seen to occur at ~12 μJ.cm^{-2} pinpointed as the lasing threshold of the dye loaded nanoparticle 1D photonic crystal, the lowest reported for a bottom-up synthetic laser.

This system provides a good example of how bottom-up colloidal and electrostatic assembly of nanoparticles and Rhodamine 6G can enable nanofabrication of an all-solid-state photonic crystal dye laser that overcomes some of the operational problems of the conventional liquid phase dye laser. Additional advantages include the ability to tune the laser wavelength by simply varying the position of the photonic band edge with respect to the dye emission. It is worth noting that following dye adsorption, much porosity is retained in the nanoparticle 1D photonic crystal thereby permitting dynamic tuning of the laser by reversible adsorption and desorption cycling of vapors and liquids[36]. This wavelength sensitivity could be enhanced by chemically anchoring surface functional groups to the constituent nanoparticles to make the laser into a molecule discriminating chemical or biological sensor.

Antibacterial silver Bragg mirror

Silver formulations have recently regained their popularity as antibacterial agents devoid of the toxic side-effects normal for other heavy-metals[37, 38]. Historically, silver in medicine can be traced as far back as Hippocrates and Plinius who first observed its efficacy in curing disease. Silver bottles were used by the Phoenicians to minimize fouling of milk, wine and water[39, 40]. The mechanism of silver's antibacterial action is conjectured to involve the binding of silver ions to reactive thiol groups in the membrane coats of bacteria causing deleterious precipitation reactions, deactivation and death[38, 41, 42].

Before the invention of antibiotics, silver compounds were used to prevent infection and various silver based creams and silver activated dressings are still utilized to heal skin wounds especially from burns[41, 42]. Other creative uses of antibacterial silver are appearing. For instance, to combat infection in hospitals, antibacterial glass coated with a layer of silver has recently been introduced. And a silver based final rinse in washing machines is considered to provide short term antibacterial protection in clothes. Silver ion embedded toilet seats are also promoted as germ killers[43, 44].

The interest in silver ion antibacterial platforms inspired us to think of a novel way of storing and releasing silver ions but with the ability to simultaneously observe the process. What came to mind was a silver ion-exchanged Bragg mirror[45]. The idea is that reflected color and time dependent color changes that originate from alterations in the effective refractive index of the layers comprising the Bragg mirror, will provide a simple and convenient optical read-out of the instantaneous silver content and the pharmacokinetic release profile of silver from the Bragg mirror[45-56].

Knowing that the antibacterial operating mechanism of silver involves targeting specific functional groups within bacterial cell membranes, the availability of silver ions over extended periods of time is a prerequisite for its sustained antimicrobial activity[38]. For the latter to be monitored *in situ*, the silver Bragg mirror optical detection system would be able to report on the silver loading state of the delivery system with respect to the antibacterial agent.

To achieve the objective of a combined silver ion storage and release platform with in situ optical detection we self-assembled Laponite clay nanoplatelets and nanoparticle or mesoporous forms of TiO$_2$ as high refractive index material to form a 1D photonic crystal that could subsequently be ion-exchanged with silver. We proceeded to show that this hierarchical construction provides access to a color-encoded silver release profile on exposure to aqueous-based solutions (Fig. 4).

The choice of the above layer materials was predicated by our previous work revealing the uptake capacity of clay-titania Bragg stacks for
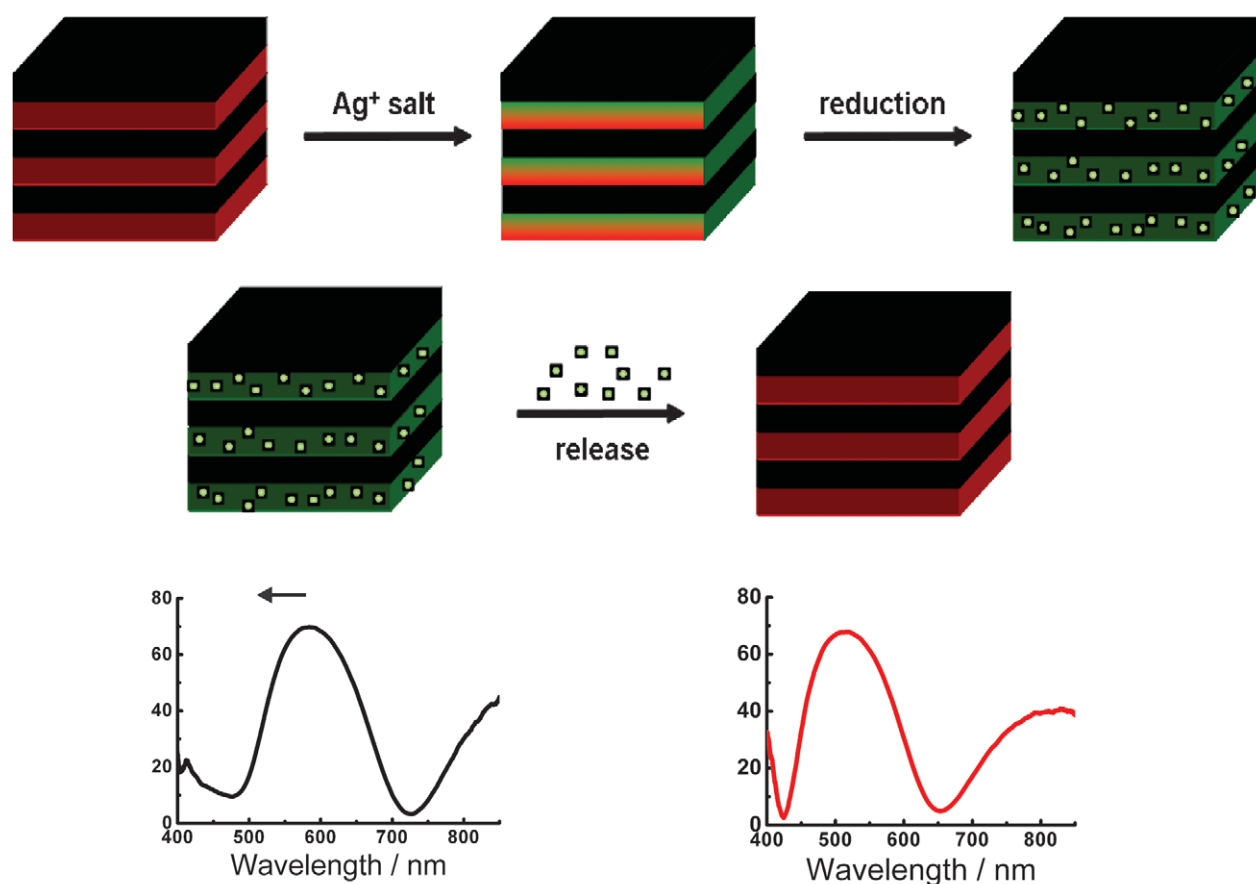
Fig. 4 *Illustration of how the structural color of 1D photonic crystals modified with silver nanoparticles by silver ion-exchange and reduction (top) is a function of the silver loading state (bottom). Silver loading and release translate into distinct changes of the stopband position in the optical spectra. Owing to their silver uptake photonic properties, clay-TiO2 Bragg stacks show potential for the detection of antimicrobial activity based on a **label-free** optical read-out system. Reproduced with permission from*[37].

various cations[52-54] and by the fact that both titania and clay distinguish themselves as non-toxic, readily available matrices with a high chemical affinity for silver ions and nanoparticles[57-59]. In addition, synergies arise from the inherent photocatalytic activity of TiO_2 on UV activation, further enhancing the antimicrobial activity of the hybrid system, and from the excellent anti-agglomeration stability of the silver nanoparticles embedded between the clay nanoplatelets and within the porous TiO_2 support[59].

The in situ exchange of sodium ions for silver ions[60] and the formation of silver nanoparticles within the photonic multilayer system can be observed by diagnostic stopband shifts of the Bragg reflected light. Remarkably, the silver ions preferentially migrate into the TiO_2 rather than the clay layers as demonstrated by X-ray photoelectron spectroscopy (XPS) depth profiles, thereby boosting the refractive index contrast and thus, the reflectivity of the Bragg stacks (Fig. 5). The slow release of silver ions provides a powerful source to impart sustained antimicrobial activity to the Bragg mirror.

The synthesis of the silver-loaded Bragg mirrors involved a two-step procedure based on wet impregnation of the layers with aqueous $AgNO_3$ solution, followed by in situ chemical or photochemical reduction of the adsorbed silver ions.

To demonstrate the antimicrobial properties of the silver Bragg mirror a disk-diffusion assay was employed to evaluate the efficacy of silver released into a bacteria colony cultured on agar. In this experiment it should be noted that the diffusion of silver ions released from silver nanoparticles by a surface oxidation mechanism as well as ion-exchanged silver both can contribute to the zone of activity given by the zone of inhibition around the sample in conformal contact with the agar medium inoculated with E. coli (Fig. 5)[37, 38]. Varying the layer thicknesses of the Bragg stacks and therefore the total amount of silver present in the multilayer system did not show any appreciable effect on the antimicrobial activity.

The overall success of this trial is considered a first step towards the practical realization of a sensing platform that combines a structural color read-out with antibacterial activity. Silver Bragg mirrors assembled from low-cost, environmentally friendly clay and titania and whose stopband position is sensitive to the state of silver loading provide exciting opportunities as label-free optical probes for antimicrobial activity when integrated into self-sterilizing wall coatings in hospitals, biocidal food containers, self-cleansing medical devices such as urinary catheters, or antimicrobial patches.
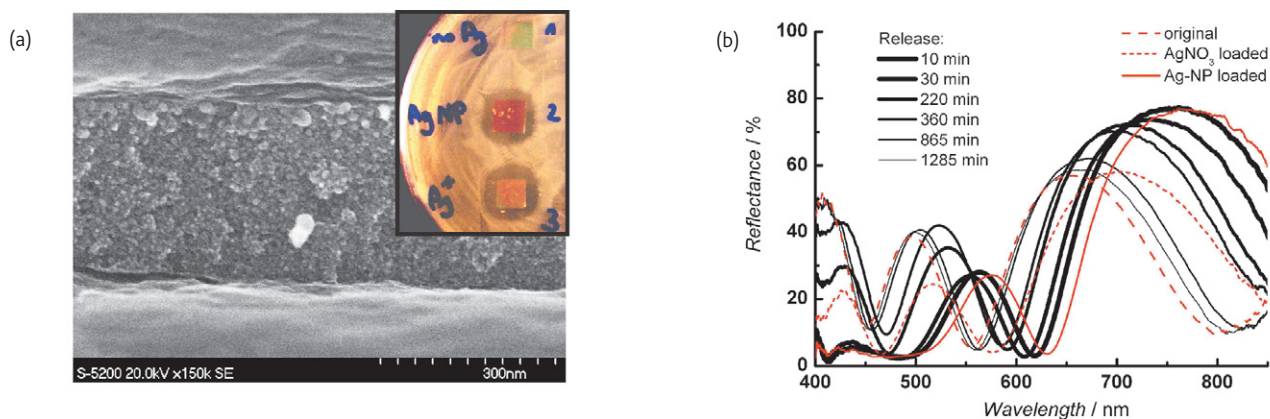
Fig. 5 *(a) SEM cross section image showing the middle meso-TiO$_2$ layer in an Ag-NP loaded (Laponite/meso-TiO$_2$)$_3$ Bragg stack. Inset: Images of the zones of inhibition observed when bringing silver Bragg mirrors face down into contact with agar plates inoculated with E. coli. 1) Original Bragg mirror, 2) with Ag-NPs, 3) impregnated with AgNO$_3$. (b) UV-vis spectra of a 3-bilayer BS during silver loading (red lines) and release (black lines) as a function of soaking time in an 1:1 ethanol/water mixture. Reproduced with permission from[37].*

3D architectures made from nanocrystals and nanowires

In recent years we developed heterogeneous reaction protocols for the synthesis of oleylamine capped lead sulfide PbS and bismuth sulfide, Bi$_2$S$_3$, nanocrystals and nanorods with diameters tuneable in the size range 4-10 nm[61-63]. The PbS nanocrystals displayed very large near infrared photoluminescence quantum yields, size dependent extinction coefficients and the narrowest recorded emission line widths[61, 62]. More recently we developed a strategy for creating ultrathin nanowires[64] of Sb$_2$S$_3$[65] and Bi$_2$S$_3$[66]. The Bi$_2$S$_3$ nanowires displayed an especially remarkable internal necklace structure, flexibility and colloidal stability. These building blocks were then all used in different fashions to fabricate self-assembled architectures through different methodologies.

In a first example, PbS and magnetic CoFe$_2$O$_4$ nanocrystals were driven into templates with pores of various dimensionalities by capillary forces (see Fig. 6)[67]. In the case of alumina membranes, the membrane was used as a filter through which a solution of nanocrystal was allowed to dry (Fig. 6b). The presence of a septum on the tube containing the liquid prevented it from flowing right through the membrane. This controlled process of evaporation led to the formation of cylindrical superlattices of nanocrystals within each channel of the template. After a cycle of nanocrystal plasma polymerization (NPP)[63, 68, 69], the template could then be removed yielding free standing one dimensional nanocrystal superlattices which could be luminescent and/or magnetic, depending on the building blocks that were originally used (Fig. 6d)[67]. A similar process was used with opals, allowing for the creation of inverse opals made of nanocrystals with luminescent and/or magnetic properties (Fig. 6e-h).[67] These processes employed capillary forces to drive the ordered assembly of nanocrystals within a template.

In the second example we used the Bi$_2$S$_3$ nanowires to make self-assembled microfibers and nanomembranes by a process we dubbed chemospinning[70]. The nanowires were flowed through a narrow gauge nozzle and injected into a solution of crosslinker in a good solvent.

The nanowires react readily with any amine at room temperature. This reactivity implies that any molecule bearing more than one amine group will crosslink the nanowires.

As shown in Fig. 7a, the process implies the real time crosslinking of the nanowire dispersion as soon as this is injected in the crosslinker solution. This leads to the formation of microfibers of tuneable thickness and porosity (Fig. 7c-e). In Fig. 7f is shown a low angle X-ray diffractogram of a deposited film of nanowires. The peaks represent different symmetries of alignment of the nanowires on the substrate. If the same experiment is conducted on the microfibers that were obtained through chemospinning the peaks get sharper indicating an increased order and alignment of the fibers (Fig. 7g). In this case the self-assembly was due to the van der Waals forces between the oleylamine ligand shells of the nanowires, and further enabled by shear alignment of the nanowires in the flow through a narrow gauge nozzle.

Dye-anchored mesoporous metal oxide electrochemiluminescent device

The templated self-assembly of myriad building blocks into a wealth of ordered porous materials has attracted intense attention in the past decade as an efficient way to produce materials with pore sizes between 2 and 50 nm[21, 71], which have, upon removal of the surfactant, potential applications in various areas, such as adsorption[72], catalysis[73], drug delivery[74], solar cells[75], optics[76] and so forth. Like other morphologies of materials, the distinctive properties of mesoporous materials are a function of the chemical and physical nature of the framework that forms the mesostructure. Therefore, a great deal of work has been devoted to synthesize mesoporous materials with various chemical compositions, such as silica, transition metal oxides, sulphides, phosphates, metals, carbon, polymers, and so on[77-79]. However, the majority of these materials are electrically insulating, which limits their applications greatly in many areas where transparency and conductivity are needed.
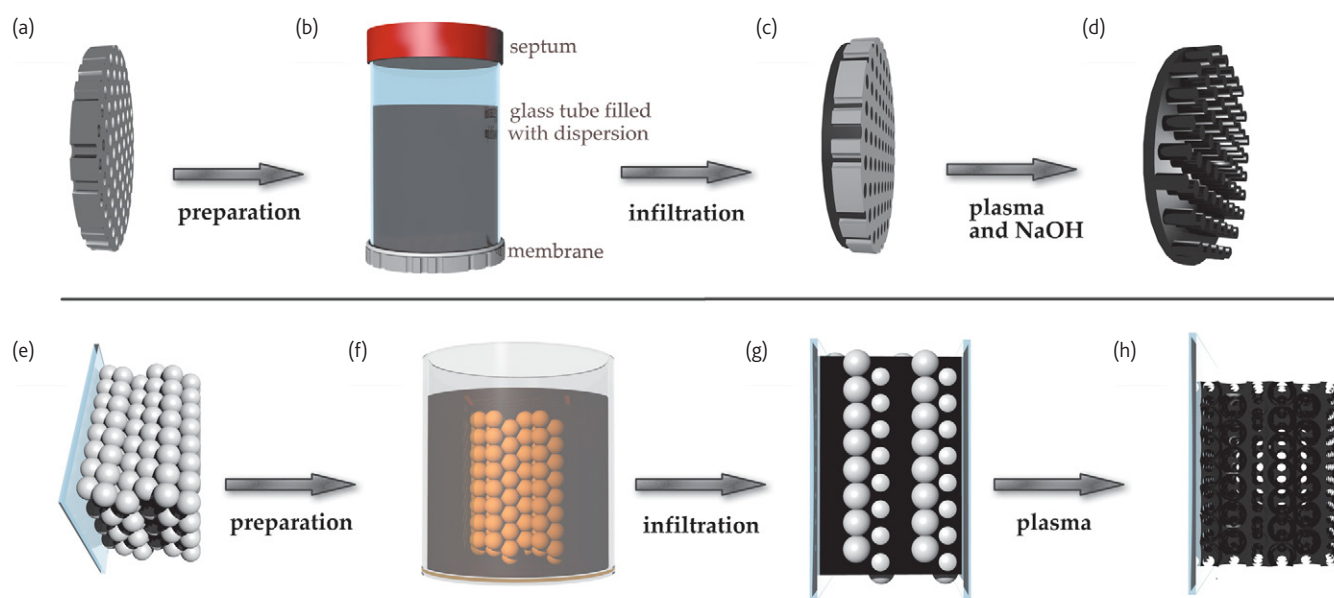
Fig. 6 *This diagram illustrates the process of self-assembly of nanocrystal dispersions into arbitrary shaped templates. On the top panel, an alumina membrane (a) is stuck at the bottom of a glass tube filled with a nanocrystal dispersion and capped with a septum (b), the capillary driven evaporation induced self-assembly of the nanocrystals produces a superlattice film of nanocrystals within the channels of the membrane (c). This material can then be liberated from the template by NPP and chemical etching of the alumina (d). In the bottom panel a polystyrene opal (e) is immersed vertically in a concentrated dispersion of nanocrystals between two glass slides (f). The evaporation of the dispersion leads to a gradual filling of the holes in the opal template (g). The nanocrystals are consolidated with a plasma by NPP which also contemporaneously removes the template (h). Reproduced with permission from[63].*

Recently we have unveiled an innovative solution to this problem with the surfactant-templated synthesis of mesoporous antimony-doped tin oxide (meso-ATO) film, a new type of electrode material that for the first time fully integrates well-ordered and high surface area mesoscale pores with high thermal stability, high electrical conductivity and high optical transparency[80]. The superior properties determined for these meso-ATO films allow the loading of a large amount of chemically anchored ruthenium dye in the mesopores, which has enabled nanofabrication of an efficient electrochemiluminescence cell (ECL), Fig. 8.

ECL is a phenomenon in which electrochemically generated reactants interact to produce light[81-83]. Among various ECL systems, the tris-bipyridyl ruthenium inorganic dye is the most widely studied because of its attractive properties, which include high ECL efficiency and good chemical and electrochemical stability under mild conditions in aqueous solutions[84].

For the ECL application, a button-cell was fabricated consisting of a dye modified meso-ATO film as the working electrode separated from a tin-doped indium oxide (ITO) counter electrode by a 4 mil Surlyn spacer. The cell was filled with electrolyte and a prescribed quantity of sacrificial co-reactant, which consisted of pH 7 phosphate-buffer and tripropylamine (TPA), respectively. After the TPA electrolyte was filled into the cell, visually bright ECL could be observed with an applied voltage of 1.1 V with respect to Ag/AgCl (NaCl) aqueous reference electrode, (Fig. 8). Dye modified dense ITO electrode was chosen as a control reference[85]. The cell using the meso-ATO film electrode,

displayed ECL emission intensity that was about 100 times higher than the cell made of dense ITO as the working electrode, for a TPA concentration of 10^{-3} M. Based on the surface area of the meso-ATO film, the estimated value of the ECL enhancement should be about 132 times, if one assumes the surface and electrical properties of meso-ATO and dense ITO are the same after treatment. In practice, the luminescence intensity of the cell should be proportional to the amount of anchored dye that can transfer electrons efficiently to the electrode. The observed enhancement is quite close to the estimated value, suggesting that the electrons transferred from the surface anchored dye permeate very efficiently in the meso-ATO framework. This implies that meso-ATO film effectively enhances the electroactive surface area compared to that of dense ITO without sacrificing desired electrode properties, such as high conductivity and high transparency.

This discovery bodes well for the use of self-assembly as a nanofabrication strategy for mesoporous antimony-doped tin oxide film for a range of optoelectronics applications from displays to lasers to biosensors.

Top-down bottom-up, which way to go?

This is a nagging question that the scientific community is constantly asking when contemplating the transfer of a nanoscience breakthrough into a scalable and manufacturable nanotechnology. In order to achieve the particular nanofabrication objectives outlined in this article it would be difficult to imagine top-down engineering physics methods that could match the bottom-up self-assembly approaches. Why is this so?
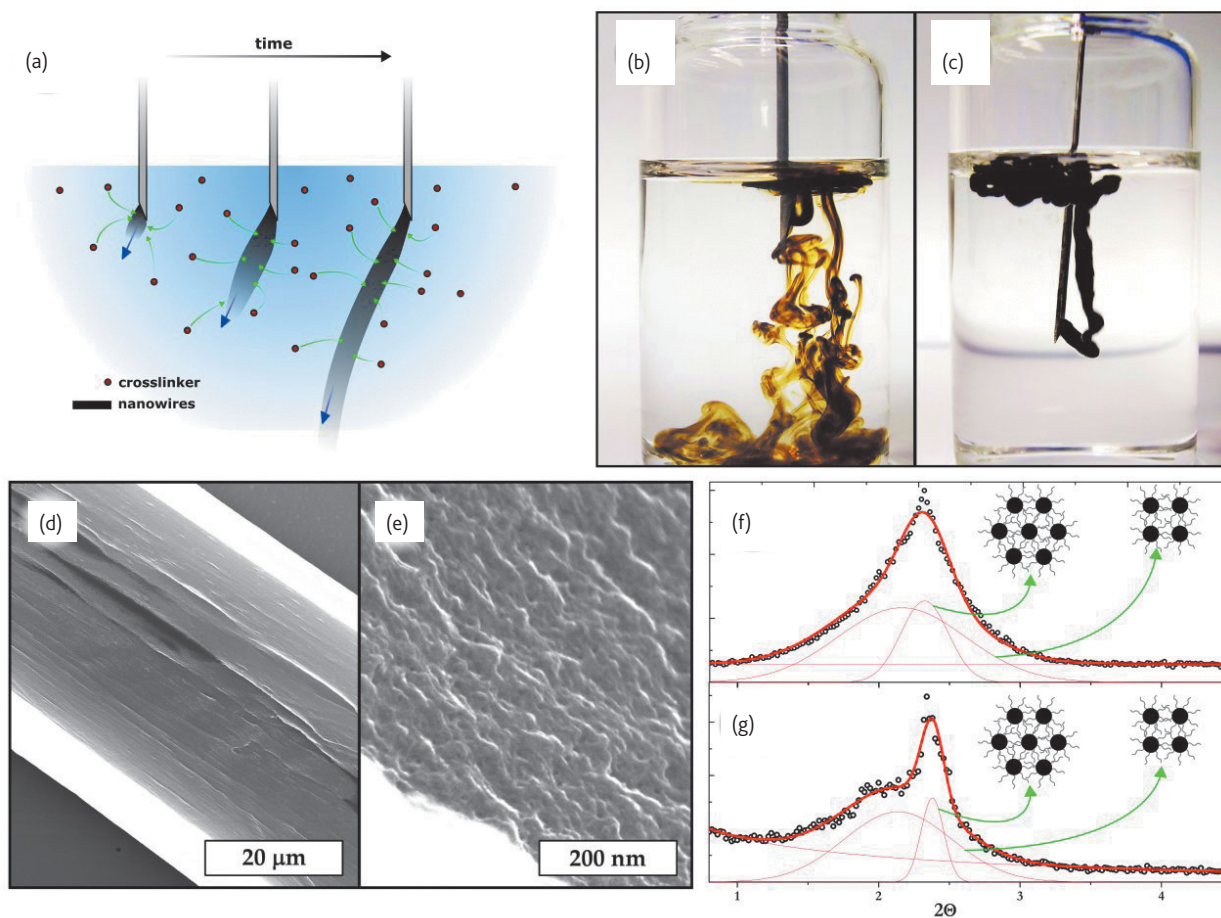
Fig. 7 *This figure displays the process of chemospinning. A dispersion of Bi$_2$S$_3$ nanowires is flowed through a narrow gauge nozzle into a solution of crosslinker (ethylene diamine). As the process develops the fibers form as the dispersion is crosslinked in contact with the solution (a). The picture in (b) and (c) show the process respectively in the absence and presence of crosslinker. The SEM micrographs in (d) and (e) show the macrostructure and microstructure of the fibers. The panels (f) and (g) show the low angle X-ray diffraction respectively of a film of Bi$_2$S$_3$ nanowires and of a film of chemospun fibers. The improvement of the alignment of the nanowires in the fibers is shown by the narrower peaks in (g). Reproduced with permission from[65]*

The success of the nanoparticle photonic crystal dye laser and the antibacterial silver Bragg mirror depended amongst other factors on the high surface area and porosity, adsorption and ion-exchange properties attainable in hierarchically assembled alternating high and low refractive index multi-layer stacks made of silica-titania and clay-titania nanoparticles, respectively. Nanofabrication of such topologically complex 3D open structures with chemically designed surfaces is readily achievable by bottom-up self-assembly but would be a challenge for top-down engineering without expensive, specialised equipment.

In the case of dye-loaded mesoporous antimony-doped tin oxide made by directed self-assembly it is the unique integration of high surface area and nanocrystalline mesoporosity together with high electrical conductivity and optical transparency that enables a ruthenium-dye based electroluminescent device to be constructed that is two orders of magnitude more efficient than the same dye adsorbed on dense indium tin oxide. Top-down engineering would have a hard time matching this feat.

Top-down nanofabrication has a long way to go before it can compete with bottom-up nanofabrication for making nanocrystal superlattices in forms like nanorods and inverse opals. Similarly it will be a long time before a top-down route can be found to match the bottom-up approach for making inorganic nanowires with diameters below 2 nm. It is the ultrathin regime between the molecular and nanoscale that imbues these nanowires with polymer-like properties and it is the ability to crosslink them with multi-dentate capping-ligands that allows the nanowires to be formed into fibers and meshes and also function as a sensitive detector for biomolecules.

Based on results from our laboratory as well as others around the world the future seems bright for nanofabrication by self-assembly.

Challenges

Where do we go from here? We have thus compiled a short list, in no specific order, of ten *scientific challenges meaningful to nanofabrication by self-assembly* for the next decade. This list is not complete neither is it set in stone but a 'living' list as objectives and priorities change with
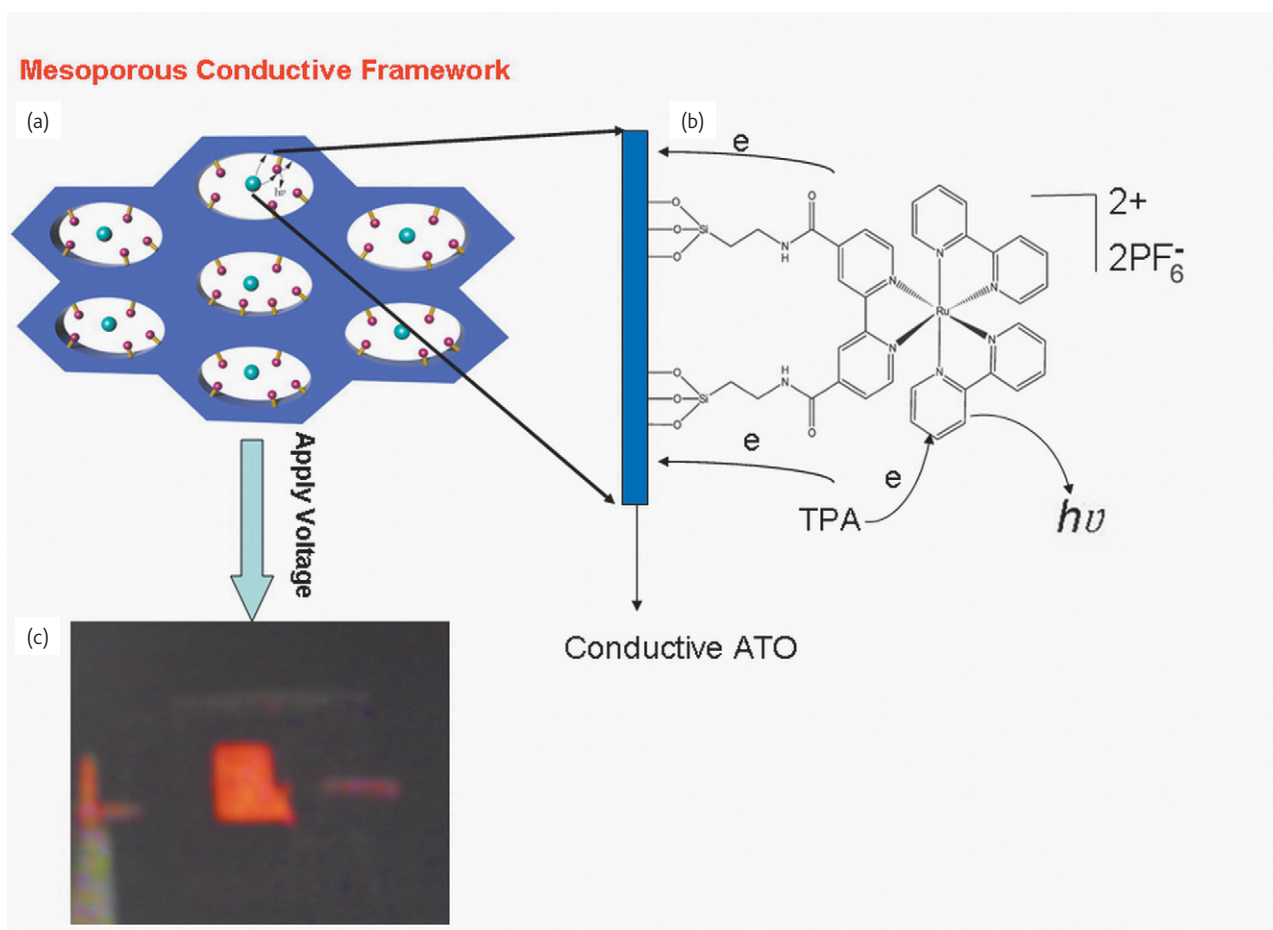
Fig. 8 (a) A ruthenium-based dye (brown) when chemically tethered to a novel high surface area conductive, transparent and well-ordered mesoporous antimony-doped tin oxide film (purple) in the presence of tripropylamine sacrificial co-reactant (blue) functions as the working electrode in a high efficiency electrochemiluminescence cell; (b) Schemes of the ECL process occurring inside the pores of the conductive meso-ATO electrode; (c) Photograph of ECL emission from meso-ATO electrode. Reproduced with permission from [80].

time being dependent on factors other than curiosity-driven science and application-driven technologies, but on geopolitical and global socioeconomic forces.

1. Cure for certain types of cancer
   a. New drug delivery agents and selective targeting strategies
   b. Novel bioconjugation techniques
2. Complete disease diagnostic system
   a. Rapid, sensitive, portable and low cost screening
3. Nanoscale electronics
   a. Nanometer precision synthesis, positioning and interconnection of building blocks
   b. Reproducible, robust and well characterized contacts
4. Solid state hydrogen storage
   a. High density, room temperature, atmospheric pressure
   b. Fast and reversible loading and unloading
5. Lightweight high energy density lithium batteries
   a. Synthesis of new solid-state battery nanomaterials
   b. Fast safe charge-discharge cycles, minimal volume swings
6. Efficient, cheap and robust solar cells
   a. Improved light harvesting panchromatic materials
   b. Enhanced photo-thermal stability of semiconductors and sensitizers
7. Highly active and selective photocatalyst
   a. Synthesis of enhanced activity photocatalytic nanomaterials
   b. Visible wavelength photocatalytic activity
8. Nanothermoelectrics
   a. Large scale synthesis of superlattice nanostructures
   b. High figure of merit refrigeration and power generation systems
9. Carbon dioxide cycling
   a. Carbon dioxide chemistry and catalysis
   b. Direct conversion to methane or methanol, ethane or ethanol
10. Abiological nanomotors
    a. Nanolocomotion, controlling speed, directionality, payload delivery
    b. Towards purposeful nanomachines

Synthetic self-assembly is but one of the enablers of nanofabrication that paves the way forward. Other indispensable players in nanofabrication include a suite of top-down lithographies, a set

nanotools for defining structure and properties of nanomaterials, nanoimaging techniques for visualizing nanostructures and nanomanipulation strategies for moving, positioning, interconnecting and contacting nanostructures.

We believe synthetic self-assembly has changed our way of thinking about new ways of using chemistry to make unprecedented structures and patterns at the nanoscale with designed function and utility. It will be fascinating to watch the field of nanofabrication by self-assembly unfold

to see if it can deliver on its promise of myriad of future nanotechnologies to improve the health and well-being of the human race and the fragile environment of planet Earth on which we all must live. `mt`

Acknowledgements

References

1. Russell, B., *A History of Western Philosophy*, Simon & Schuster (1972).
2. Langmuir, I., and Blodgett, K. B., *Kolloid-Zeitschrift* (1935) **73**, 257.
3. Bigelow, W. C., *et al.*, *J. Coll. Sci.* (1946) **1**, 513.
4. Nuzzo, R. G., and Allara, D. L., *J. Am. Chem. Soc.* (1983) **105**, 4481.
5. Laibinis, P. E., *et al.*, *J. Am. Chem. Soc.* (1991) **113**, 7152.
6. Troughton, E. B., *et al.* *Langmuir* (1988) **4**, 365.
7. Love, J. C., *et al.*, *Chem. Rev.* (2005) **105**, 1103.
8. Xia, Y. N., and Whitesides, G. M., *Ann. Rev. Mater. Sci.* (1998) **28**, 153.
9. Keller, S. W, *et al.*, *J. Am. Chem. Soc.* (1994) **116**, 8817.
10. Lvov, Y., *et al.*, *J. Am. Chem. Soc.* (1995) **117**, 6117.
11. Lvov, Y., *et al.*, *Langmuir* (1993) **9**, 481.
12. Chan, W. C. W., and Nie, S., *Science* (1998) **281**, 2016.
13. Bruchez, Jr. M., *et al.* , *Science* (1998) **281**, 2013.
14. Friedman, R. S., *et al.*, *Nature* (2005) **434**, 1085.
15. Khang, D. Y, *et al.*, *Science* (2006) **311**, 208.
16. Lopez, C., *et al.*, *Adv. Mater.* (2003) **15**, 1679.
17. Zakhidov, A. A., *et al.*, *Science* (1998) **282**, 897.
18. Tang, C. B., *et al.*, *Science* (2008) **322**, 429.
19. Whitesides, G. M., and Grzybowski, B., *Science* (2002) **295**, 2418.
20. Cademartiri, L., and Ozin, G. A., *Concepts of Nanochemistry,* Wiley-VCH (2009).
21. Kresge, C. T., *et al.*, *Nature* (1992) **359**, 710.
22. Sakurai, M., *et al.*, *Langmuir* (2007) **23**, 10788.
23. Aizenberg, J., *et al.*, *Phys. Rev. Lett.* (2000) **84**, 2997.
24. Ginger, D. S., *et al.*, *Angew. Chem. Int. Ed.* (2004) **43**, 30.
25. Fialkowski, M., *et al.*, *J. Phys. Chem. B* (2006) **110**, 2482.
26. Scotognella, F., *et al.*, *Small* (2009), accepted.
27. Akahne, Y., *et al.*, *Nature* (2003) **425**, 994.
28. Shkunov, M. N., *et al.*, *Adv. Funct. Mater.* (2002) **12**, 21.
29. Kogelnik, H., and Shank, C. V., *Appl. Phys. Lett.* (1971) **18**, 152.
30. Kogelnik, H., and Shank, C. V., *J. Appl. Phys.* (1972) **43**, 2327.
31. Dowling, J. P., *et al.*, *J. Appl. Phys.* (1994) **75**, 1896.
32. Zhai, L., *et al.*, *Macromolecules* (2004) **37**, 6113.
33. Colodrero, S., *et al.*, *Langmuir* (2008) **24**, 4430.
34. Shank, C. V., *et al.*, *Appl. Phys. Lett.* (1970) **353**, 737.
35. Montalti, M., *et al.*, in *Handbook of Photochemistry* (3rd ed.), Taylor & Francis, Boca Raton FL (2006), p. 325.
36. Colodrero, S., *et al.*, *Langmuir* (2008) **24**, 9135.
37. Lotsch, B. V., *et al.*, *Small* (2009), DOI: 10.1002/smll.200801925.
38. Lee, D., *et al.*, *Langmuir* (2005) **21**, 9651.
39. Holleman, A. F., and Wiberg, E., *Lehrbuch der Anorganischen Chemie* (101st ed.), Walter de Gruyter, New York (1995), p. 1338.
40. Angelotti, N., and Martini, P., *Minerva medica* (1997) **88**, 49.
41. Atiyeh, B., *et al.*, *Burns* (2007) **33**, 139.
42. Lansdown, A. B. G., *Curr. Probl. Dermat.* (2006) **33**, 17.
43. http://www.glassglobal.com/news/agc_flat_glass_europe_launches_first_antibacterial_glass-7232.html
44. http://www.saltlakemetals.com/Silver_Antibacterial.htm
45. Wang, T. C., *et al.*, *Adv. Mater.* (2002) **14**, 1534.
46. Li, Y. Y., *et al.*, *Science* (2003) **229**, 2045.
47. Choi, S. Y., *et al.*, *Nano Lett.* (2006) **6**, 2456.
48. Fuertes, M. C., *et al.*, *Adv. Funct. Mater.* (2007) **17**, 1247.
49. Convertino, A., *et al.*, *Adv. Mater.* (2003) **15**, 1103.
50. Fuertes, M. C., *et al.*, *Phys. Chem. C* (2008) **112**, 3157.
51. Snow, P. A., *et al.*, *J. Appl. Phys.* (1999) **86**, 1781.
52. Lotsch, B. V., and Ozin, G. A., *Adv. Mater.* (2008) **20**, 4079.
53. Lotsch, B. V., and Ozin, G. A., *ACSNano* (2008) **2**, 2065.
54. Bonifacio, L. D., *et al.*, *Adv. Mater.* (2009) **21**, 1.
55. Lee, D., *et al.*, *Nano Lett.* (2006) **6**, 2305.
56. Wu, Z., *et al.*, *Small* (2007) **3**, 1445.
57. He, J., *et al.*, *Chem. Commun.* (2002), 1910.
58. Fuertes, M. C., *et al.*, *Small* (2009) **5**, 272.
59. Liu, J., *et al.*, *Colloid. Surf. A* (2007) **302**, 276.
60. Czímerová, A., *et al.*, *J. Coll. Interf. Sci.* (2007) **306**, 316.
61. Cademartiri, L., *et al.*, *J. Phys. Chem. B* (2006) **110**, 671.
62. Cademartiri, L., *et al.*, *J. Am. Chem. Soc.* (2006), **128**, 10337.
63. Malakooti, R., *et al.*, *Adv. Mater.* (2006) **18**, 2189.
64. Cademartiri, L., and Ozin, G. A., *Adv. Mater* (2009) **21**, 1013.
65. Malakooti, R., *et al.*, *J. Mater. Chem.* (2008) **18**, 66.
66. Cademartiri, L., *et al.*, *Angew. Chem. Int. Ed.* (2008) **47**, 3814.
67. Ghadimi, A., *et al.*, *Nano Lett.* (2007) **7**, 3864.
68. Cademartiri, L., *et al.*, *Small* (2005) **1**, 1184.
69. Cademartiri, L., *et al.*, *Acc. Chem. Res.* (2008) **41**, 1820.
70. Cademartiri, L., *et al.*, *Nano Lett.* (2009) **9**, 1482.
71. Beck, J. S., et al., *J. Am. Chem. Soc.* (1992) **114**, 10834.
72. Hartmann, M., *Chem. Mater.* (2005) **17**, 4577.
73. Melero, J. A., *et al.*, Chem. Rev. (2006) **106**, 3790.
74. Vallet-Regi, M., *Chem. Eur. J.* (2006) **12**, 5934.
75. Hou, K., *et al.*, J. *Mater. Chem.* (2005) **15**, 2414.
76. Scott, B. J., *et al.*, *Chem. Mater.* (2001) **13**, 3140.
77. Soler-IIlia, G. J. A. A., *et al.*, *Chem. Rev.* (2002) **102**, 4093.
78. Liang, C., *et al.*, *Angew. Chem. Int. Ed.* (2008) **47**, 2.
79. Wan, Y., *et al.*, *Chem. Rev.* (2007) **107**, 2821.
80. Hou, K., *et al.*, *Adv. Mater.* (2009), DOI: 10.1002/adma.200803330.
81. Pyati, R., and Richter, M. M., *Annu. Rep. Prog. Chem., Sect. C* (2007) **103**, 12.
82. Richter, M. M., *Chem. Rev.* (2004) **104**, 3003.
83. Tokel, N. E., and Bard, A. J., *J. Am. Chem. Soc.* (1972) **94**, 2862.
84. Tokel-Takvoryan, N. E., *et al.*, *J. Am. Chem. Soc.* (1973) **95**, 6582.
85. Mian, W. J., *et al.*, *J. Am. Chem. Soc.* (2002) **124**, 14478.